

Nucleation and Growth Behavior of Twin Region Around Yield Point of Polycrystalline Pure Ti

G. Murasawa · T. Morimoto · S. Yoneyama

Received: 18 January 2011 / Accepted: 17 May 2011 / Published online: 4 June 2011
© Society for Experimental Mechanics 2011

Abstract The aim of the present study is to investigate the nucleation and growth behavior of twin region around yield point of polycrystalline pure Ti under deformation. Firstly, we prepare commercial polycrystalline pure Ti plate, and investigate the microstructure and pole figures using an Electron Backscatter Diffraction Patterns device. Secondly, tensile specimens are cut out from 0°, 30°, 45° and 90° relative to plate rolling direction. Then, we measure the macroscopic stress–strain curve, local strain distribution and nucleation and growth of twin region arising in specimens under uniaxial tensile loading. Results show the anisotropic characteristics in those behaviors. Those could be related to *c* axis in hcp lattice. However, detailed anisotropic mechanism may have something to do with several interactions between slips and twins arising in its body. It is also understood that the avalanche behavior of twin region nucleation occurs as a result of larger twin region formation, with inhomogeneous small twin region nucleation in transient process. Finally, we could suppose the bridge mechanism of deformation behaviors from macroscale to microscale for polycrystalline pure Ti under deformation.

Keywords Polycrystalline pure Ti · Yield point · Avalanche · Twin region · Digital image correlation · Acoustic emission

G. Murasawa (✉, SEM member) · T. Morimoto
Department of Mechanical Engineering, Yamagata University,
4-3-16, Jonan,
Yonezawa, Yamagata 992-8510, Japan
e-mail: murasawa@yz.yamagata-u.ac.jp

S. Yoneyama (SEM member)
Department of Mechanical Engineering,
Aoyama Gakuin University,
5-10-1, Fuchinobe,
Sagamihara, Kanagawa 229-8558, Japan

Introduction

Macroscopic deformation behavior is governed by nucleation or growth behaviors of slip and twin for polycrystalline metal materials. The behaviors of slip and twin usually reveal the phenomena such as intermittent deformation behavior [1], spatial clustering and avalanche behavior [2–4], and self-similar or scale free [5] under deformation. In recent years, Weiss et al., Uchic et al. and Poulsen et al. have studied about the intermittent deformation behavior arising in solid materials. Weiss et al. have measured the motion of slip for single- and poly- crystalline ice under creep deformation using acoustic emission technique. They have reported that the motion of slip showed avalanche behavior and its behavior is different between single- and poly- crystalline [2–6]. Furthermore, Richeton et al. have conducted AE experiments during plastic deformation of hcp metallic single crystals. They have reported that dislocation avalanches in relation with slip and twinning were identified with the only sources of AE and a power law relation was in perfect agreement with one previously found in ice single crystals [7]. Uchic et al. have fabricated the micro order compressive specimen of pure Ni by focused ion beam process. Then, they have conducted uniaxial compression test using a nanoindentation device. They have reported that the slip behavior showed scale free phenomenon [1, 8, 9]. Also, Poulsen et al. have reported the unexpected intermittent dynamics such as appearing and disappearing with proceeding deformation and even displaying transient splitting behavior during tensile deformation of pure Cu [10]. Above-mentioned phenomena are much important topics for elucidating the mechanism of plastic deformation in polycrystalline metal materials.

The unit cell of pure Ti is hexagonal close-packed structure. For single crystal pure Ti, it is reported that

$\{10\bar{1}2\}$ twin can be observed when basal plane has the angle of 78° for the direction of tensile loading at 22°C , whereas $\{11\bar{2}1\}$ twin and a little prism slip can be observed when the angle of basal plane is 47° for the direction of tensile loading at -195°C [11]. In general, it is known that $\{10\bar{1}2\}$, $\{11\bar{2}1\}$, and $\{11\bar{2}3\}$ twins allow an extension along the c axis, while $\{11\bar{2}2\}$, $\{10\bar{1}1\}$, and $\{11\bar{2}4\}$ twins permit a reduction [12]. For polycrystalline pure Ti, it is reported that $\{10\bar{1}2\}$ twin or $\{11\bar{2}2\}$ twin can be observed at room temperature [13–16].

The aim of the present study is to investigate the nucleation and growth behavior of twin region around yield point of polycrystalline pure Ti under deformation. Firstly, we prepare commercial polycrystalline pure Ti plate, and investigate the microstructure and pole figures using an Electron Backscatter Diffraction Patterns (EBSD) device. Secondly, tensile specimens are cut out from 0° , 30° , 45° and 90° relative to plate rolling direction. Then, we measure the macroscopic stress–strain curve, local strain distribution and nucleation and growth of twin region arising in specimens under uniaxial tensile loading. In this time, the in-house measurement system, which the present authors produce for integration with the tensile machine control system, local strain distribution measurement system and twin region measurement system, is constructed suited on a Lab VIEW platform. Local strain distribution is measured by in-house system on the basis of Digital Image Correlation (DIC). Also, the nucleation and growth of twin region are measured by in-house other one on the basis of acoustic emission (AE) technique. Finally, we discuss about nucleation and growth mechanism of twin region around yield point of polycrystalline pure Ti under deformation, on the basis of results in present study.

Material and Methods

Material

Material is commercial polycrystalline pure Ti plate (99.5%, 1 mm thickness, The Nilaco corporation). An optical image of microstructure and pole figures for $\{0001\}$, $\{10\bar{1}2\}$ and $\{11\bar{2}2\}$ planes are obtained from EBSD device. Tensile specimens are cut out from 0° , 30° , 45° and 90° relative to plate rolling direction as shown in Fig. 1(a). Figure 1(b) shows specimen configuration. The titanium tabs are attached to the specimen by epoxy resin. Random pattern is created on the specimen surface by spraying black and white paint for measuring strain distribution by DIC method.

Measurement Method of Local Strain Distribution

DIC software is in-house one, and the details of DIC are reported in the references [17, 18]. In these references,

Yoneyama et al. proposed a principal method and its algorithm of DIC. Also, they have applied this method to measurement of stress intensity factor around crack tip [18] and bridge deflection [19]. A test system, local strain distribution measurement system, is also constructed on the basis of DIC as an in-house software suited on a Lab VIEW platform. We can semi-automatically measure strain distribution using the system. Its details are presented in the references [20, 21].

Measurement Method of Twin Region Nucleation

AE is a powerful technique for investigating nucleation or growth of slip and twin during deformation. AE signals are generated by dislocation glide or twinning. Thus, we can measure the number of nucleation and nucleation speed for twin region during deformation. Also, some researchers have reported that the amplitudes of AE signals are related to the area swept by the fast-moving slip and hence to the energy dissipated during deformation events [6, 22]. Thereby we assume that twin region size is corresponding to the amplitude of AE signals, and measure it.

AE signal measurement

AE signals are monitored using four small AE sensors. Four small AE sensors are aligned on a center straight line on the specimen surface as shown in Fig. 1(c). In present experiment, No.1 and No.4 sensors are used as guard sensor, and No.2 and No.3 sensors are as effective sensor for acquiring AE signals only from effective area. The method used is the following. (1) Four AE signals are monitored for a event during measurement, (2) Arrival times (No.1 sensor: t_1 , No.2 sensor: t_2 , No.3 sensor: t_3 , No.4 sensor: t_4) are recorded from the AE signals, (3) In the case of $t_1 > t_2$ and $t_4 > t_3$, AE signals are regarded as a signal from effective area. These processes are automatically conducted during measurement by in-house software suited on a Lab VIEW platform.

Figure 2 shows a typical AE signal monitored from No.2 and No.3 sensors for a event. For each event, wave analysis allows us to record two parameters, the arrival time t_0 (the time at which the signal reaches threshold value A_{\min}) and the maximum amplitude A_0 . Recording is automatically conducted for all data by in-house wave analysis software suited on a Lab VIEW platform.

Cumulative AE event counts (the number of twin region nucleation) and AE event count rate (the twin region nucleation speed)

Cumulative AE event count—time relations are obtained from detected AE signals. Furthermore, AE event count



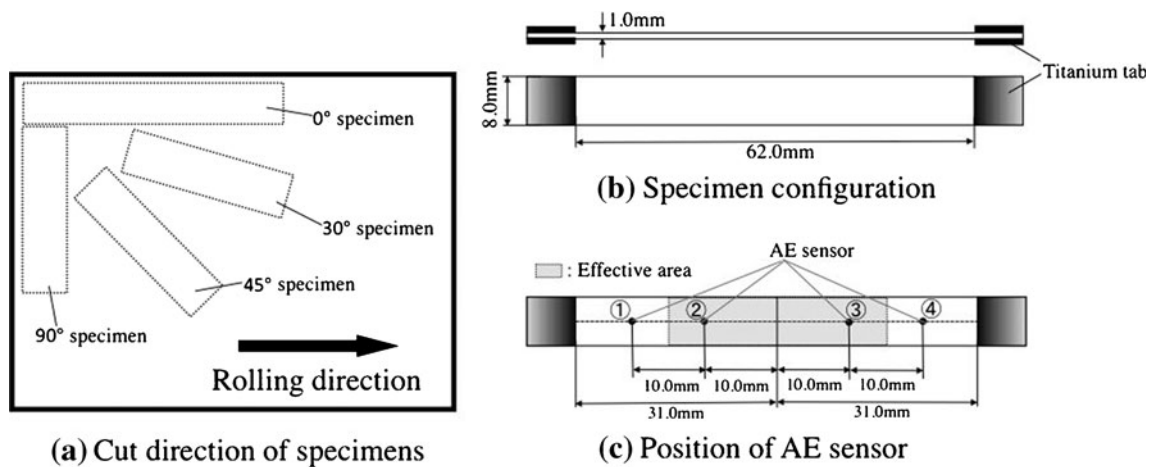


Fig. 1 Specimen configuration

rate—time relation can be calculated from the cumulative AE event count—time curves. The calculation method of AE event count rate is shown in Fig. 3. Firstly, an arbitrary point x_0 is determined from the points on the cumulative AE event count—time curve, and its before and after points, 50 points, are selected as shown in Fig. 3(a) and (b). Secondly, these 51 points are approximated by quadratic least squares method. Thirdly, the slope of approximated quadratic curve is obtained at the point x_0 as shown in Fig. 3(b). The slope value is AE event count rate at the point x_0 . Finally, this calculation is conducted at all points on cumulative AE event count—time curve. Then, we can obtain AE event count rate—time relation as shown in Fig. 3(c). Calculation is automatically conducted for all data by in-house data analysis software suited on a Lab VIEW platform.

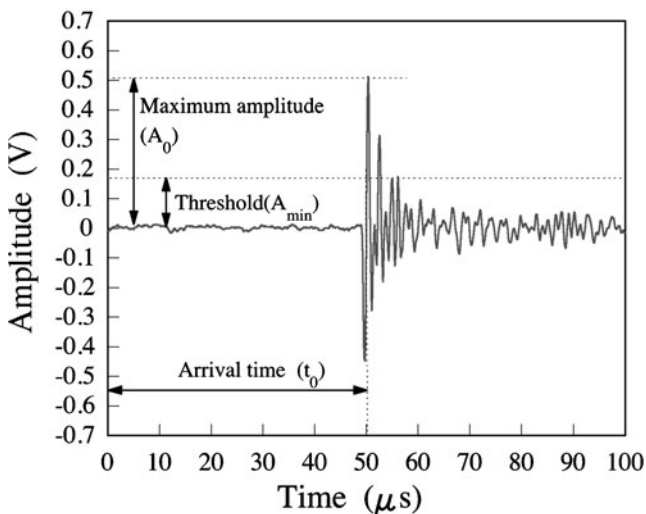


Fig. 2 Detected AE wave

Experimental Setup of In-House Measurement System Integrated with Local Strain Distribution and AE Measurements

Uniaxial tensile loading is performed for specimens at room temperature (21°C). Autograph (AGS-5KNG, Shimadzu) is used in present test. The strain rate is 0.08%/min. A CCD camera (HC-HR70, Sony) is set in front of the specimen. A 50 mm lens (VCL-50Y-M, Sony) is attached to the CCD camera. The specimen images are taken into computer every 5 s during tensile loading. Four small AE sensors with frequency bandwidth of 300 kHz–2 MHz (AE-900 M, NF corporation) are mounted on another surface of specimen. The output signals are amplified 40 dB by the pre-amplifier (9916, NF corporation) and then 20 dB by the discriminator (AE9922, NF corporation), and fed to an oscilloscope and a computer. We set the proper threshold value (0.3 mV) for AE signal. In this time, the noise amplitude is 0.08 mV. Data are sampled at an interval of 100 ns. Also, we use the computer with a GPIB interface (NI GPIB-USB-HS, National Instrument) to control tensile machine, a monochrome PCI frame grabber (mvTITAN-G1, Matrix Vision) to acquire 1024×768 8-bit grayscale digital image from the CCD camera and two 12-bit AD converters (PCI-3163, Interface) to acquire AE signals from four AE sensors. Then, the in-house software integrated with tensile machine control system, local strain distribution measurement system and twin region measurement system is constructed suited on a Lab VIEW platform.

Results

Microstructure of Polycrystalline Pure Ti

Figure 4(a) depicts an optical image of microstructure for present Ti. Also, Fig. 4(b) presents the pole figures for

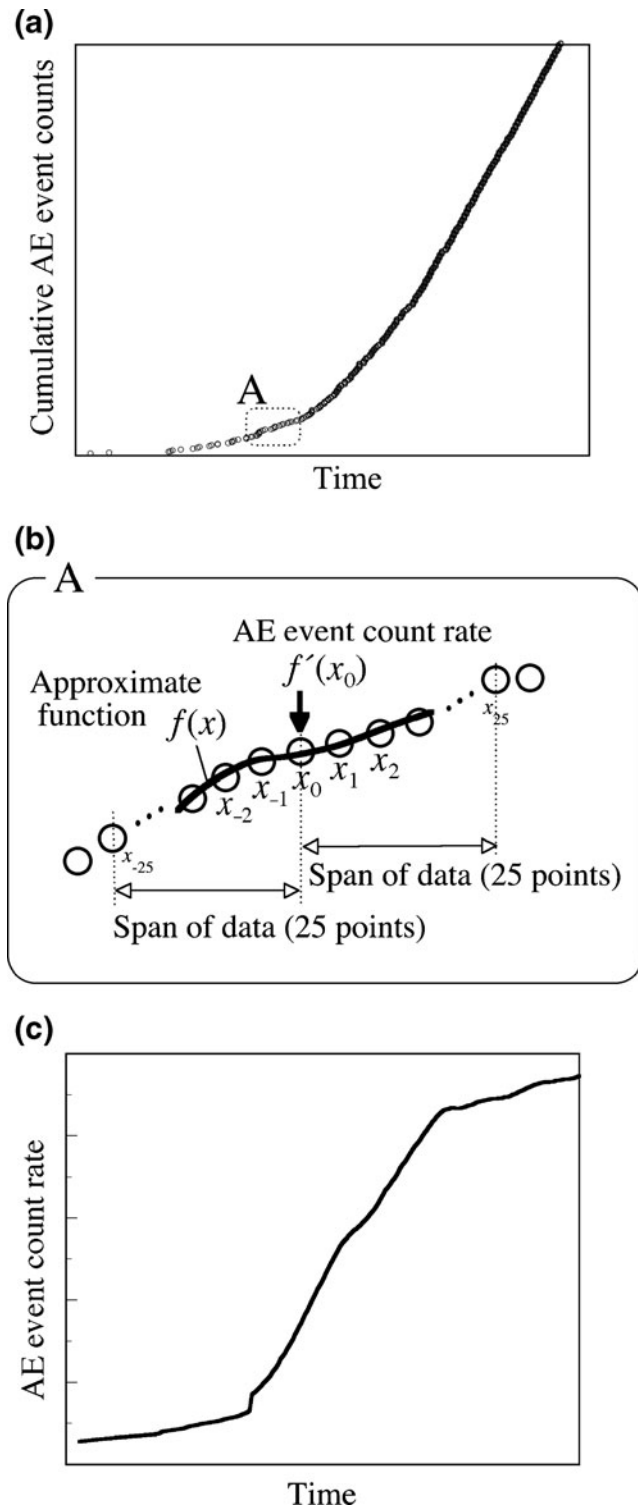


Fig. 3 Method of the AE event count rate calculating. (a) cumulative event AE counts-time curve obtained from AE monitoring system (b) the methods for the approximation of cumulative AE event counts-time curve and calculation of AE event count rate (c) AE event count rate - time curve

$\{0001\}$, $\{10\bar{1}2\}$ and $\{11\bar{2}2\}$ planes. As shown in these figures, we can see some residual slips or twins as a result of cold rolling. c axis inclines from ND direction to TD direction, and hexagonal close-packed structure spins at the position.

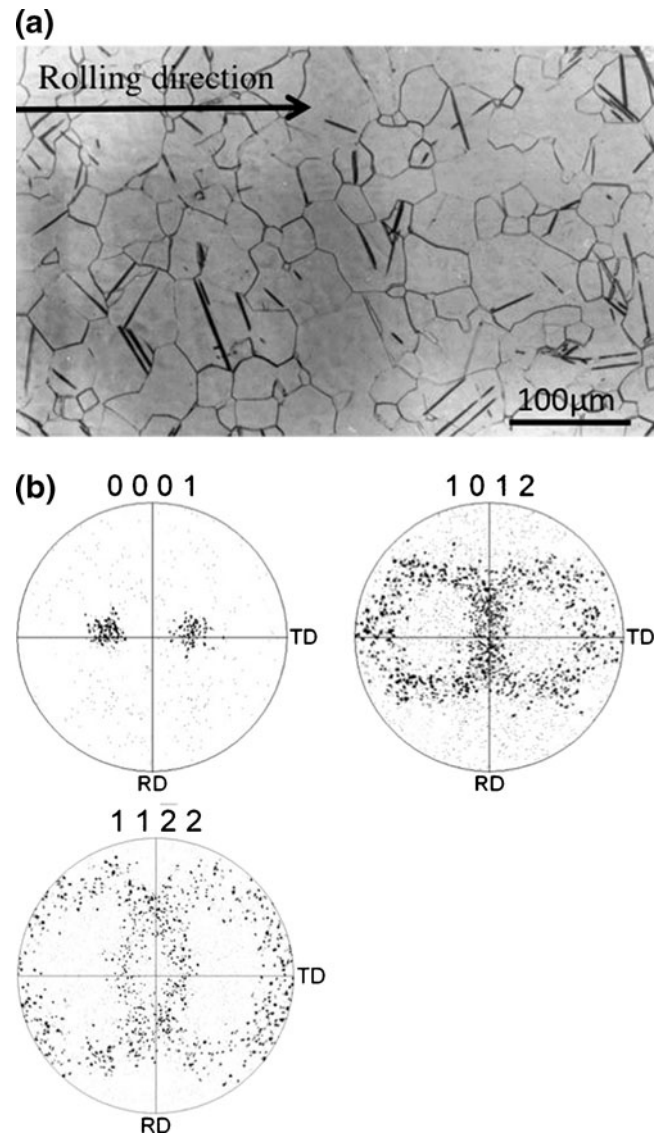


Fig. 4 Microstructure (a) and pole figures (b) of polycrystalline pure Ti

Macroscopic Stress–Strain Curves of Polycrystalline Pure Ti

Figure 5 portrays macroscopic stress–strain curves for the specimens which are cut out from 0° , 30° , 45° and 90° relative to plate rolling direction. From these results, it is seen that 0° specimen result shows the same behavior with 30° specimen result. In contrast, 45° specimen result shows a little larger yield stress and flow stress than that of 0° and 30° specimens. Additionally, 90° specimen result shows more larger ones than others.

Local Strain Distribution Around Yield Point of Polycrystalline Pure Ti

Figure 6(a)–(d) demonstrate stress-time curve and longitudinal local strain distribution for 0° , 30° , 45° and 90°

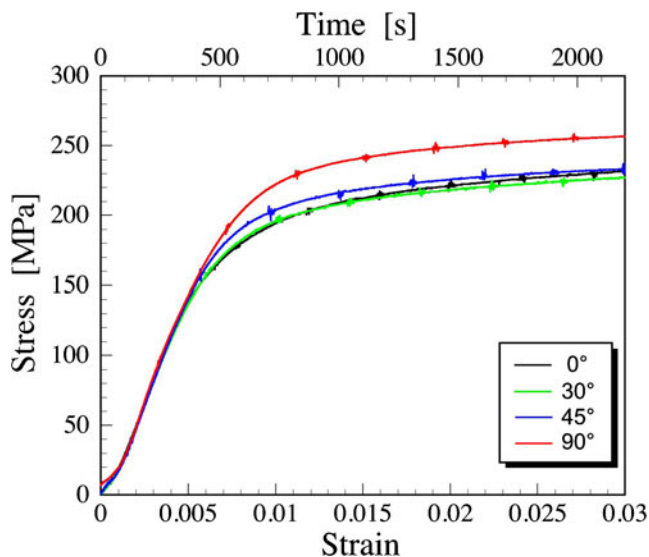


Fig. 5 Macroscopic stress–strain curves of polycrystalline pure Ti

specimens. Local strain distribution is measured at the times indicated as (1)–(12) in Fig. 6. The strain value is shown in right hand scale level in Fig. 6. The longitudinal and transversal axes in Fig. 6 show the position on picture used in DIC, which are along to x (horizontal axis) direction and y (vertical axis) direction in picture. From even a cursory examination of Fig. 6(a)–(d), it is seen that all specimen results reveal inhomogeneous strain distribution, and the cluster of local strain gradually increase around yield point of stress–strain curve. In addition, the cluster nucleation of local strain depends on the cut direction of specimen. It becomes late from 0° to 90° .

Twin Region Nucleation Around Yield Point of Polycrystalline Pure Ti

Figure 7 gives stress–time curves, cumulative AE event count–time curves and AE event count rate–time curves around yield point for all specimens under tensile loading. As presented in the result of AE event count rate–time curves, it can be seen that 0° and 30° specimen results show the avalanche behavior of twin region nucleation around yield point. 0° specimen result especially presents the drastic avalanche behavior around the early stage of yield point. Additionally, the twin region nucleation speed becomes equilibrium state from latter stage of yield point. In contrast, the twin region nucleation does not appear around the early stage of yield point for 45° and 90° specimens. Then, their specimen results show small avalanche behavior at the latter stage of yield point or the beginning stage of plastic deformation, as compared with former ones.

Discussion

Mechanism of Twin Region Nucleation

Twin region nucleation is strongly governed by grain orientation in Ti [14, 15]. Changes of stress system and of specimen orientation have been shown to produce a variety of twin structures in Ti sheet metal and other hcp sheet metals. These variations will be discussed in the terms of the interaction of the imposed stress system with the crystallographic texture of the metal, and of the contrasts between polycrystalline sheet metal and single crystal behavior [14, 16, 23–28]. For hcp metals, a length change along the c axis can also be accomplished by twinning. In single crystal Ti, it is known that $\{10\bar{1}2\}$, $\{11\bar{2}1\}$, and $\{11\bar{2}3\}$ twins allow an extension along the c axis, while $\{11\bar{2}2\}$, $\{10\bar{1}1\}$, and $\{11\bar{2}4\}$ twins permit a reduction [12]. In polycrystalline pure Ti, it is reported that $\{10\bar{1}2\}$ twin or $\{11\bar{2}2\}$ twin can be observed at room temperature [13–16].

Figure 4(b) presents the pole figures for $\{0001\}$, $\{10\bar{1}2\}$ and $\{11\bar{2}2\}$ planes of present Ti plate. From Fig. 4(b), the results show that $\{0001\}$ plane strongly indicates anisotropy for the in-plane direction. The c axis inclines from ND direction to TD direction, and is transverse to specimen rolling direction. In uniaxial tension at room temperature, 0° specimen contains $\{11\bar{2}2\}$ twin as a result of c axis compression. In 90° specimen, $\{10\bar{1}2\}$ twin appears, activated by c axis tension [14, 15]. Present experimental results obviously show the anisotropic characteristics in the macroscopic stress–strain curve, local strain distribution and twin region nucleation behavior. We can assume that these characteristics may result not only from twin nucleation as a result of c axis orientation but also from several interactions between slips and twins. In fact, Paton et al. have reported that metallographic examination of the deformed single crystals Ti revealed only $\{11\bar{2}2\}$ twins under compression parallel to the c axis, and copious prism slips appeared in addition to $\{10\bar{1}2\}$ twins under compression perpendicular to the c axis at room temperature [12]. Furthermore, Yoo has reported the interaction between slips and twins in deformed polycrystalline hcp metals [13]. The interaction between slips and twins provides much important information for elucidating the plasticity of hcp metal, thereby measuring the interactions would be necessity for us.

Mechanism for the Avalanche Behavior of Twin Region Nucleation

Bulatov et al. have assumed from their numerical results that various inelastic processes in solids have a common microscopic origin, i.e., local inelastic transformations involving relatively small pieces of solid structure [29]. In

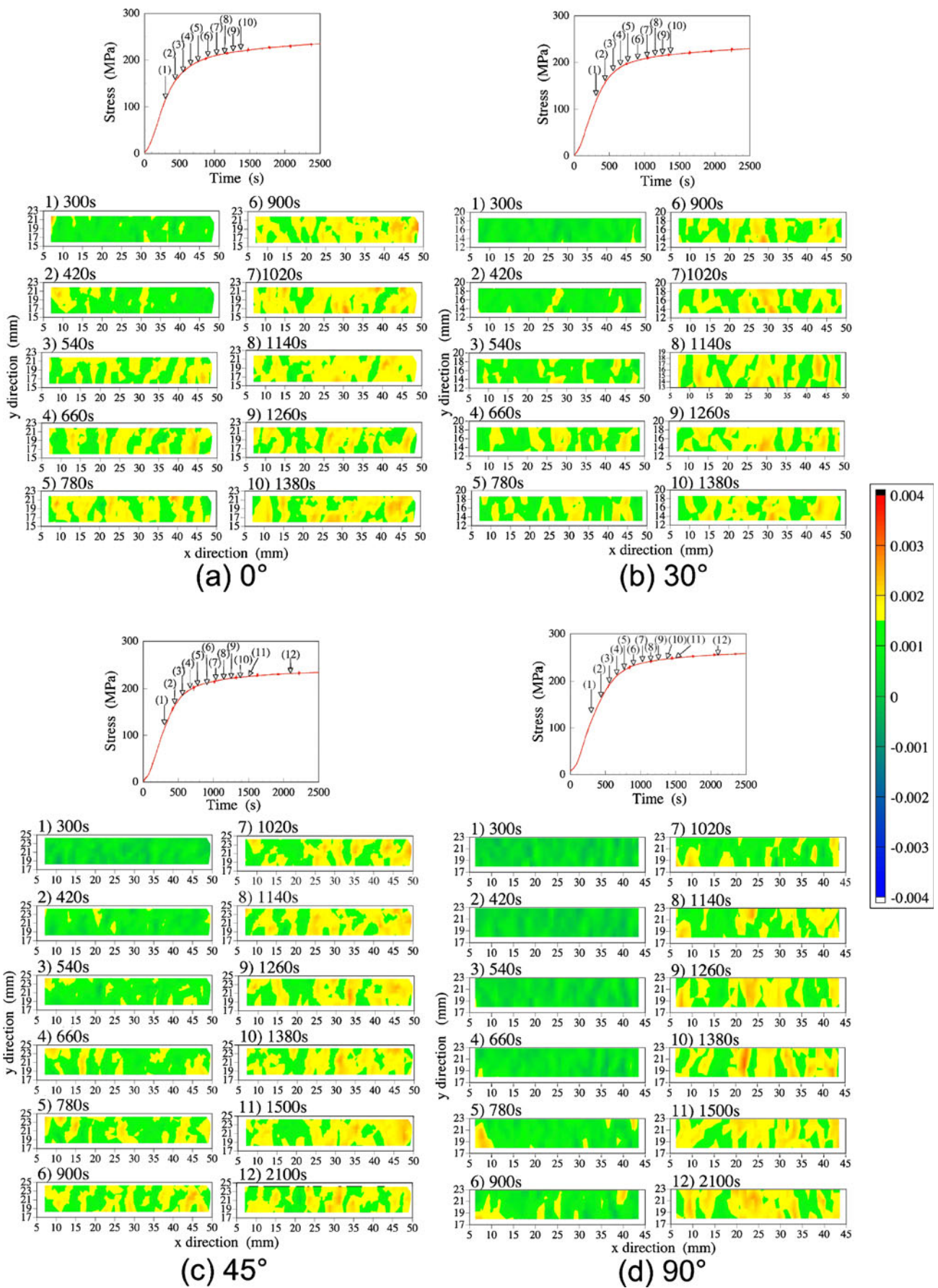


Fig. 6 Longitudinal strain distribution of polycrystalline pure Ti under uniaxial tensile loading (a) 0° specimen, (b) 30° specimen, (c) 45° specimen, (d) 90° specimen

fact, a twin region measured as an AE signal consists of some twinned grains, and some twin regions form a cluster of local strain in macroscopic level. Thereby we can notice that such a deformation process has something to do with the origin for avalanche behavior of twin region nucleation. AE event counts are considered as the number of twin region, and it is assumed that AE signal amplitudes are related to the twin region size. From these measurement data, we try to discuss about the mechanism for avalanche behavior of twin region nucleation. Here, AE signals occur as a result of twin reorientation in a grain. However, the AE event counts during twin reorientation are found to be one or two orders of magnitude lower than during nucleation [30]. Therefore, AE event counts as a result of twin reorientation are not considered in present experiment.

Growth of twin region

Figure 8 displays the amplitude distributions obtained from AE signals for polycrystalline pure Ti under tensile loading.

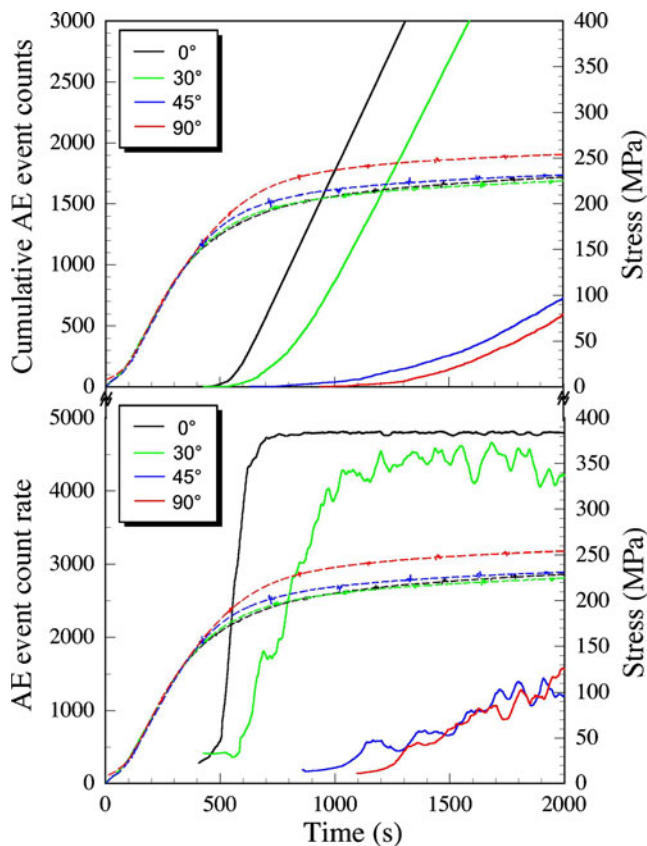


Fig. 7 Cumulative AE event count—time curves and AE event count rate—time curves of polycrystalline pure Ti under uniaxial tensile loading

Additionally, Fig. 8(a)–(d) show the results which specimens are cut out from 0°, 30°, 45° and 90° relative to plate rolling direction. Maximum voltage is detected for each AE signal, and that is related to the twin region size for each event. Figure 8(a)–(d) also demonstrate the results for each 250 event counts up to 2,000 event counts during deformation. From these figures, we can see that all specimens have a lot of twin regions from small size to large size for each 250 event counts. In addition, it can be seen that the distribution at the latter stage of event counts depends on the cut direction. In the case of nearly 0° specimen, larger twin region size increases during deformation. These facts imply that a small twin region formation occurs, and its subsequent formation into a large twin region happens. Furthermore, it can be seen from Figs. 7 and 8 that the percentage of larger twin region size drastically increases after the equilibrium state of nucleation speed. This means that the interaction between nucleated smaller twin regions influences on the formation of a larger twin region. That is to say, twin coalescence or increase in local stress affecting the twin growth may occur. In contrast, the size distribution of twin region is almost constant during deformation in the case of nearly 90° specimen. This means that the interaction between twin regions does not occur, thereby the formation of a larger twin region does not appear.

Avalanche behavior

0° specimen demonstrates the drastic avalanche behavior of twin region nucleation. In addition, larger twin regions happen in deformed 0° specimen. This implies that the avalanche behavior occurs as a result of the larger twin region formation. Figure 9 shows a schematic illustration of twin region growing process. The twin region size transits from smaller size distribution state to larger size distribution state around yield point. In the transition process of 0° specimen, twin regions may nucleate with inhomogeneous like Fig. 9(a). Thereby twin region size change drastically happens. On the other hand, twin regions nucleate with relatively homogeneous like Fig. 9(b) in the transition process of 90° specimen. In this time, twin region size change calmly happens.

It is much important for us to study about “how does the twinning behave in polycrystalline pure Ti under deformation”. The related studies [8, 10, 29, 31] conclude that the deformation of crystals having highly mobile dislocations exhibits the attributes of a self-organized critical process [32, 33]. For example, Bulatov et al. have proposed the numerical approach to account for various common features of plastic flow in solids, and to compare the kinetics of simulated plasticity in ordered and disordered solid under similar loading conditions. They have investigated the

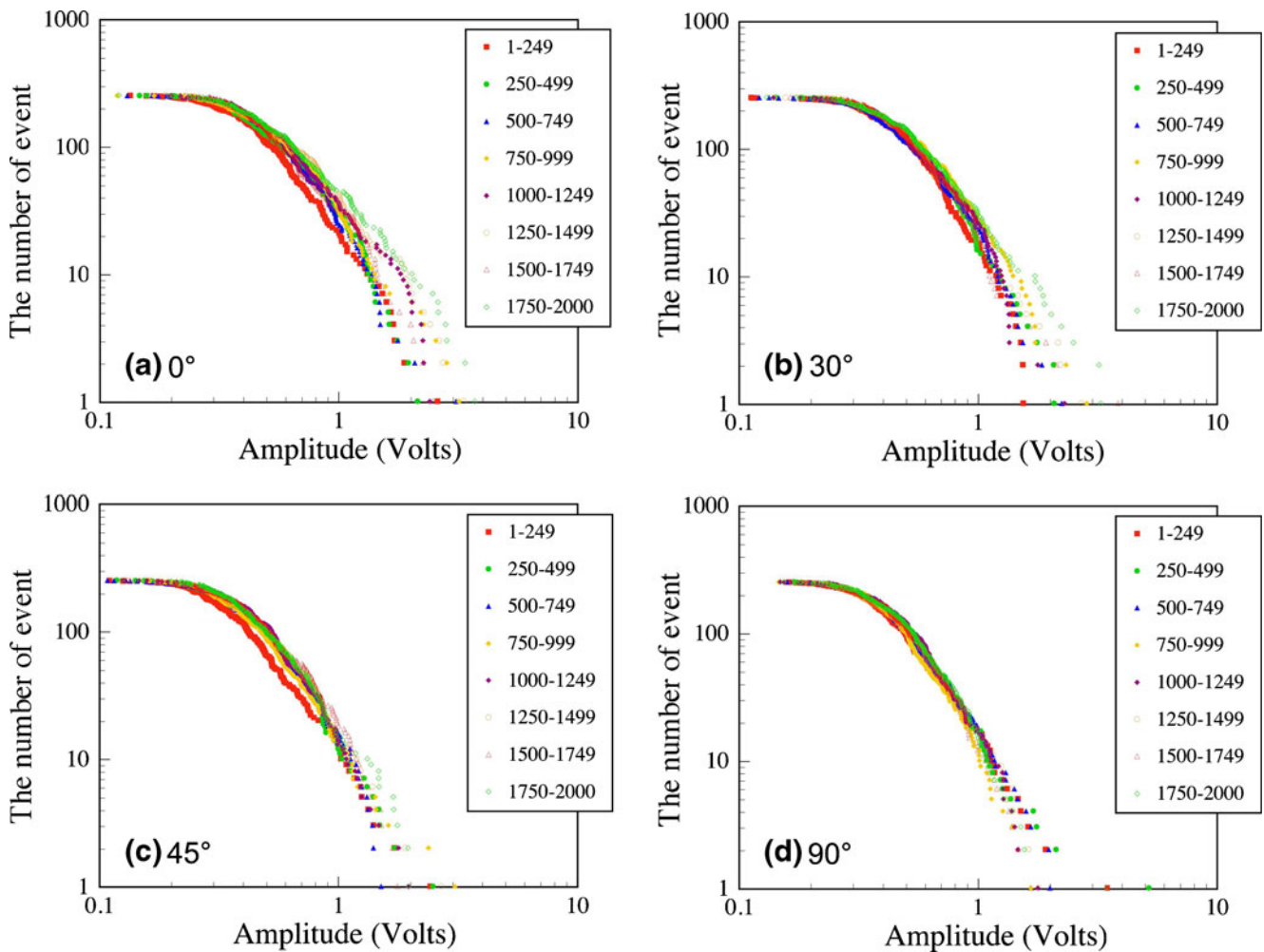


Fig. 8 AE amplitude distributions for each 250 counts of polycrystalline pure Ti under uniaxial tensile loading. (a) 0° specimen, (b) 30° specimen, (c) 45° specimen, (d) 90° specimen

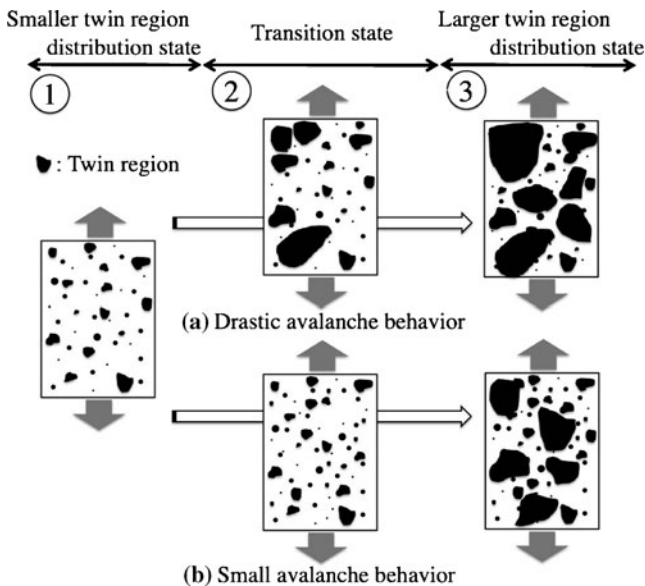


Fig. 9 Schematic illustration of twin region growing process for polycrystalline pure Ti under deformation

relationship between macroscopic stress–strain curve and local inelastic transformations occurring in small volume elements. Thereby different initial structural states showed that the character of plastic flow in transients was strongly affected by the degree of initial disorder [29]. In addition to present results, it is much interesting for us to discuss about the nucleation and growth of twin region based on such a self-organized critical process. However, the studies about the spatial information in the nucleation and growth of twin region are future work.

The Bridge Mechanism of Deformation Behaviors from Macroscale to Microscale

We could measure the cluster of local strain at macroscale, and nucleation and growth behaviors of twin region at subscale for polycrystalline pure Ti under deformation. As a result, following bridge mechanism of deformation behaviors from macroscale to microscale can be supposed.

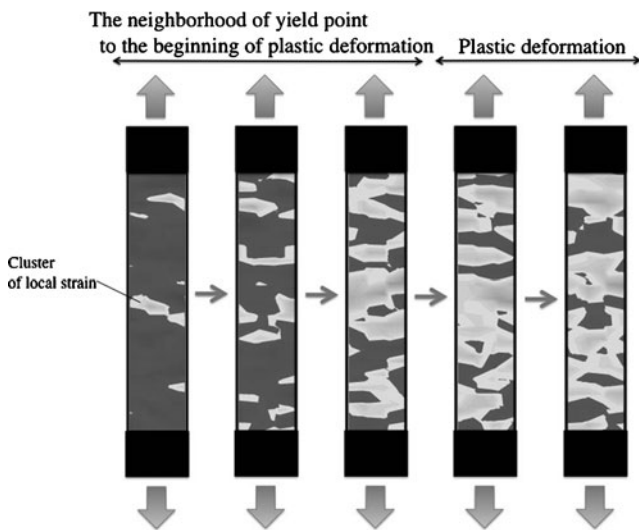


Fig. 10 Macroscopic inhomogeneity arising in polycrystalline pure Ti under uniaxial tensile loading

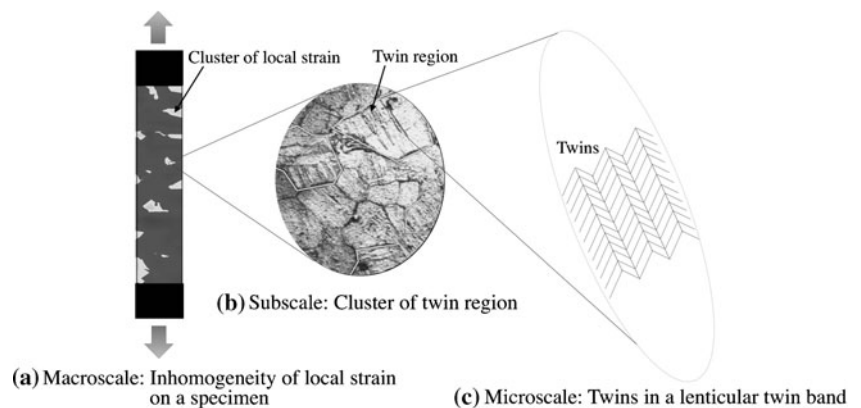
(1) Macroscale deformation behavior

Figure 10 shows the schematic illustration of macroscopic inhomogeneity arising in polycrystalline pure Ti under uniaxial tensile loading. As you can see this illustration, the clusters of local strain begin to appear around yield point. The cluster drastically increases up to the beginning of plastic deformation. Then, the increase of clusters becomes constant under plastic deformation.

(2) Subscale and microscale deformation behavior

Figure 11 illustrates the bridge mechanism of deformation behaviors from macroscale to microscale for polycrystalline pure Ti under uniaxial tensile loading. As illustrated in Fig. 11, a macroscopic cluster of local strain consists of a lot of twin regions. Additionally, the nucleation and growth of twin region behave with intermittent, scale invariant, avalanche and spatial clustering at subscale. A twin region consists of some twinned grains. At microscale, a twin in a grain nucleates and grows during deforma-

Fig. 11 The bridge mechanism of deformation behaviors from macroscale to microscale for polycrystalline pure Ti under deformation



tion. Here, a twin is formed as lenticular shape and zigzag shape of crystal structures. Also, a twin can grow in a grain as a result of twin reorientation after nucleation under deformation.

Conclusions

Firstly, we prepared commercial polycrystalline pure Ti plate, and investigated the microstructure and pole figures. Secondly, tensile specimens were cut out from 0°, 30°, 45° and 90° relative to plate rolling direction. Then, we measured the macroscopic stress–strain curve, local strain distribution and nucleation and growth of twin region arising in specimens under uniaxial tensile loading. Obtained results are the following.

- (1) From the results of macroscopic stress–strain curves, 45° specimen result displays a little larger yield stress and flow stress than 0° and 30° specimen results. 90° specimen result shows more larger ones than others.
- (2) From the results of local strain distribution, all specimen results reveal inhomogeneous deformation behavior. In addition, the cluster of local strain gradually increase around yield point of stress–strain curve. Furthermore, the cluster nucleation of local strain depends on the cut direction of specimen, and it becomes late from 0° to 90°.
- (3) From the results of the nucleation and growth of twin region, 0° and 30° specimen results show the avalanche behavior of twin region nucleation around yield point. 0° specimen result especially demonstrates drastic avalanche behavior. Additionally, the nucleation speed of twin region becomes equilibrium state after showing avalanche behavior. In contrast, the twin region nucleation does not appear around yield point for 45° and 90° specimens. Then, their specimens gives small avalanche behavior at the latter stage of yield point or the beginning stage of plastic deformation, as compared with former ones.

Results showed the anisotropic characteristics in macroscopic stress–strain curve, local strain distribution and twin region nucleation behavior. Those could be related to c axis in hcp lattice. However, detailed anisotropic mechanism may have something to do with several interactions between slips and twins arising in its body. It was also understood that drastic avalanche behavior of twin region nucleation might occur as a result of larger twin region formation, with inhomogeneous small twin region nucleation in transient process. Finally, we could suppose the bridge mechanism of deformation behaviors from macroscale to microscale.

Acknowledgements The author would like to express my deep gratitude to Prof. Mitsutoshi Kuroda (Yamagata University, Japan), Associate Prof. Takuya Uehara (Yamagata University, Japan) and Assistant Prof. Kengo Yoshida (Yamagata University, Japan) for fruitfully discussing about present study. Also, The author would like to express my deep gratitude to Dr. Tadaaki Satake (Yamagata University, Japan), Mr. Masato Obata and Mr. Naotaka Tobita for the help of experiments.

References

- Dimiduk DM, Woodward C, LeSar R, Uchic MD (2006) Scale-free intermittent flow in crystal plasticity. *Science* 312(5777):1188–1190
- Weiss J, Marsan D (2003) Three-dimensional mapping of dislocation avalanches: clustering and space/time coupling. *Science* 299(5603):89–92
- Richeton T, Weiss J, Louchet F (2005) Breakdown of avalanche critical behaviour in polycrystalline plasticity. *Nat Mater* 4(6):465–469
- Richeton T, Weiss J, Louchet F (2005) Dislocation avalanches: Role of temperature, grain size and strain hardening. *Acta Mater* 53(16):4463–4471
- Miguel MC, Vespignani A, Zapperi S, Weiss J, Grasso JR (2001) Intermittent dislocation flow in viscoplastic deformation. *Nature* 410(6829):667–671
- Weiss J, Grasso J (1997) Acoustic emission in single crystals of ice. *J Phys Chem B* 101(32):6113–6117
- Richeton T, Dobron P, Chmelik F, Jerome W, Louchet F (2006) On the critical character of plasticity in metallic single crystals. *Mater Sci Eng A* 424(1–2):190–195
- Dimiduk DM, Uchic MD, Parthasarathy TA (2005) Size-affected single-slip behavior of pure nickel microcrystals. *Acta Mater* 53(15):4065–4077
- Uchic MD, Dimiduk DA (2005) A methodology to investigate size scale effects in crystalline plasticity using uniaxial compression testing. *Mater Sci Eng A* 400:268–278
- Jakobsen B, Poulsen HF, Lienert U, Almer J, Shastri SD, Sorensen HO, Gundlach C, Pantleon W (2006) Formation and subdivision of deformation structures during plastic deformation. *Science* 312(5775):889–892
- Akhtar A (1975) Basal slip and twinning in α -titanium single crystals. *Metall Trans A* 6A:1105–1113
- Paton N (1970) Plastic deformation of titanium at elevated temperatures. *Metall Trans A* 1(10):2839–2847
- Yoo MH (1981) Slip, twinning and fracture in hexagonal close-packed metals. *Metall Trans A* 12(3):409–418
- Mullins S, Patchett BM (1981) Deformation microstructures in titanium sheet-metal. *Metall Trans A* 12(5):853–863
- Battaini M, Pereloma EV, Davies CHJ (2007) Orientation effect on mechanical properties of commercially pure titanium at room temperature. *Metall Trans A* 38A(2):276–285
- Christian JW, Mahajan S (1995) Deformation Twinning. *Prog Mater Sci* 39(1–2):1–157
- Yoneyama S, Morimoto Y (2003) Accurate displacement measurement by correlation of colored random patterns. *JSME Int J Series A - Solid Mech Mater Eng* 46(2):178–184
- Yoneyama S, Morimoto Y, Takashi M (2006) Automatic evaluation of mixed-mode stress intensity factors utilizing digital image correlation. *Strain* 42(1):21–29
- Yoneyama S, Kitagawa A, Iwata S, Tani K, Kikuta H (2007) Bridge deflection measurement using digital image correlation. *Exp Tech* 31(1):34–40
- Murasawa G, Yoneyama S, Sakuma T (2007) Nucleation, bifurcation and propagation of local deformation arising in NiTi shape memory alloy. *Smart Mater Struct* 16(1):160–167
- Murasawa G, Kitamura K, Yoneyama S, Miyazaki S, Miyata K, Nishioka A, Koda T (2009) Macroscopic stress-strain curve, local strain band behavior and the texture of NiTi thin sheets. *Smart Mater Struct* 18(5):055003
- Pollock A (1973) Acoustic emission-2: acoustic emission amplitudes. *Non-Destr Test* 6(5):264–269
- Agnew SR, Yoo MH, Tome CN (2001) Application of texture simulation to understanding mechanical behavior of Mg and solid solution alloys containing Li or Y. *Acta Mater* 49(20):4277–4289
- Agnew SR, Duygulu O (2005) Plastic anisotropy and the role of non-basal slip in magnesium alloy AZ31B. *Int J Plasticity* 21(6):1161–1193
- Proust G, Tome CN, Kaschner GC (2007) Modeling texture, twinning and hardening evolution during deformation of hexagonal materials. *Acta Mater* 55(6):2137–2148
- Proust G, Tome CN, Jain A, Agnew SR (2009) Modeling the effect of twinning and detwinning during strain-path changes of magnesium alloy AZ31. *Int J Plasticity* 25(5):861–880
- Kalidindi S (2004) A crystal plasticity framework for deformation twinning in continuum scale simulation of eng. materials: fundamentals-microstructures-process applications. In: Raabe D, Roters F, Barlat F, Chen LQ (eds) Ch27:543–560
- Staroselsky A, Anand L (2003) A constitutive model for hcp materials deforming by slip and twinning: application to magnesium alloy AZ31B. *Int J Plast* 19(10):1843–1864
- Bulatov VV, Argon AS (1994) A stochastic-model for continuum elastoplastic behavior. 3. Plasticity in ordered versus disordered solids. *Model Simul Mater Sci* 2(2):203–222
- Toronchuk JP (1977) Acoustic emission during twinning of zinc single crystals. *Mater Eval* 35(10):51–53
- Ananthakrishna G, Noronha SJ, Fressengeas C, Kubin LP (1999) Crossover from chaotic to self-organized critical dynamics in jerky flow of single crystals. *Phys Rev E* 60(5):5455–5462
- Bak P, Tang C, Wiesenfeld K (1987) Self-organized criticality—an explanation Of $1/f$ Noise. *Phys Rev Lett* 59(4):381–384
- Bak P, Tang C, Wiesenfeld K (1988) Self-organized criticality. *Phys Rev A* 38(1):364–374